J. Fluid Mech. (1969), *vol.* 38, *part* 1, *pp.* 161–179
Printed in Great Britain

On the outer-edge problem of a hypersonic boundary layer

By RICHARD S. LEE

McDonnell Douglas Astronautics Company-Western Division, Santa Monica, California

AND H. K. CHENG

University of Southern California, Los Angeles, California

(Received 17 September 1968 and in revised form 13 February 1969)

Existing analytical treatments of the hypersonic strong interaction problem adopt the two-region structure of the classical boundary-layer theory; however, the uneven heating and external vorticity created by the highly curved, leading-edge shock wave leads to the question of the uniform validity of the boundary-layer approximation near the boundary-layer edge. Recently Bush (1966), using a non-linear viscosity-temperature law ($\mu \propto T^{\omega}$, $\omega < 1$) instead of the linear one ($\mu \propto T$) used by previous investigators, demonstrated the need to analyze separately a transitional layer intermediate between the inviscid region and the boundary layer. In this paper, an asymptotic analysis of the Navier–Stokes equations in von Mises's variables, allowing a three-region structure, is carried out for the case of $\mu \propto T$. Results, with the second-order effects associated with heating and vorticity accounted for, show that a separate analysis of the transitional region is not strictly necessary in this case, and hence the equivalence of the two-region approach is confirmed. On the other hand, it is shown that the second-order boundary-layer correction owing to the heating and vorticity effects, not considered by Bush, is necessary in order to determine a uniformly valid temperature distribution in the physical variables. Numerical results for an insulated and a cold flat plate, considerably different from those of others, are obtained.

1. Introduction

The classical boundary-layer formulation was employed by Lees (1953) to study the strong interaction between a hypersonic boundary layer over a flat plate and its associated inviscid flow, with two modifications. One modification is the simultaneous determination of the boundary layer and its induced pressure, which is certainly the essence of interaction. The other is the assumption of a vanishing temperature at the outer edge of the boundary layer, which implies a sharp outer edge and is justifiable in view of the high temperature level attained in a hypersonic boundary layer. This assumption so simplifies the analysis that self-similar solutions for both the inviscid region and the boundary layer were obtained by Stewartson (1955).

A physical feature in this problem which is absent in classical boundary-layer flows is the strong and highly curved shock wave near the leading edge, which heats the inviscid flow unevenly and creates an external vorticity. The self-similar solution for the inviscid region shows that both the temperature and vorticity tend to become infinite near the boundary-layer edge. The self-similar solution for the boundary layer, on the other hand, does not provide a temperature and vorticity behaviour near the outer edge to match. Lees (1956) showed that this heating and vorticity effect calls for a higher-order boundary-layer correction which is more important in order of magnitude than the classical corrections (Van Dyke 1962). Subsequently Oguchi (1958) attempted to refine Lees's estimate of this correction by solving the higher-order boundary-layer problem exactly and was able to show that the higher-order solution does provide a temperature and vorticity behaviour near the outer edge to match the inviscid solution. Unfortunately, errors make his results unreliable. Moreover, like Lees, he used the tangent-wedge formula to calculate the correction on the induced pressure and the boundary-layer thickness. This is a poor approximation for either a monotomic or a diatomic gas as an investigation of the higher-order inviscid problem will show. Recently, Matveeva & Sychev (1965) also studied the heating and vorticity effect using an inverse approach.

Accurate results obtained systematically for the higher-order correction owing to the heating and vorticity effect in a direct problem therefore remain to be given. They are, practically speaking, by no means unimportant and are objectives of the present study. However, our main concern in this paper is a more important basic theoretical point, untouched by previous studies, namely the validity of the boundary-layer solution near the outer edge or, in other words, the applicability of the two-region flow-field structure assumed in these studies. It can be shown that in the boundary layer the leading temperature approximation decays exponentially while its higher-order correction decays algebraically; hence the leading boundary-layer approximation must fail from the asymptotic viewpoint somewhere near the outer edge and possibly also all the higher-order approximation. A related point is the 'sharpness' of the outer edge. One can expect, in connexion with the heating and vorticity correction, that the sharp outer edge should really be treated as a layer thinner than the boundary layer, and that the temperature (and the vorticity) behaviour undergo rapid transition in this layer. There is naturally an associated displacement effect of this layer on the neighbouring flow regions. Recently, Bush (1966) showed that a transitional layer, intermediate between the inviscid region and the boundary layer, has to be analyzed separately in order to obtain a uniformly valid first approximation for temperature. However, without the higher-order correction in the boundary layer and the inviscid region, his solution must be considered incomplete, since the location of streamlines in the transitional layer, even to the first approximation, is dependent on the higher-order boundary-layer displacement effect. Furthermore, he used a non-linear viscosity–temperature law ($\mu \propto T^{\omega}$, $\omega < 1$) instead of the linear one ($\mu \propto T$) used by others. It should not be surprising if the form of the viscosity–temperature law has some influence on the flow structure of the viscous regions.

In what follows, we develop an asymptotic analysis from the Navier–Stokes equations in von Mises's variables for a perfect gas obeying a linear viscosity–temperature law. In order to resolve our main concern about uniform validity, the flow field bounded by a semi-infinite flat plate and its attached shock wave is allowed to be composed of three distinct regions: an inviscid hypersonic small-disturbance region, a transitional layer and a boundary layer. Asymptotic expansions of the flow quantities, including the higher-order correction owing to the heating and vorticity effect, are carried out in each of the regions, in terms of a small parameter which represents the order of magnitude of the boundary-layer thickness.

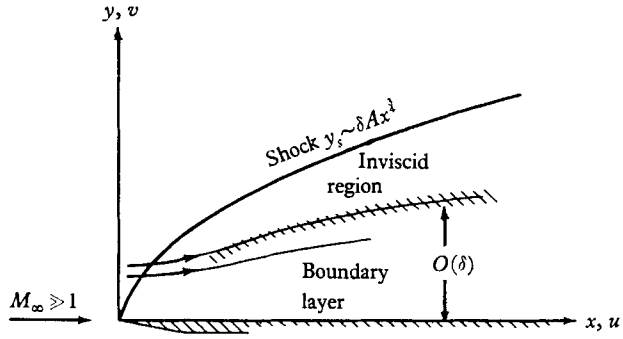

FIGURE 1. Sketch of hypersonic strong interaction over a flat plate. Hatched area between the inviscid region and the boundary layer represents the transitional layer. The solid curves with an arrowhead represent streamlines.

Matching of these expansions is executed in established overlapping regions of validity. The successful treatment of the transitional layer depends on the introduction of a proper variable. Explicit results obtained therefrom show that the valid asymptotic solution is exactly the leading boundary-layer approximation plus its higher-order correction. Thus we confirm the validity of the two-region structure in this case on the basis of a more rigorous, asymptotic analysis and elucidate the flow field near the outer edge. We also show by the results that the heating and vorticity effect is not only an important correction in the inviscid region and the boundary layer, but also a necessary consideration in achieving an unambiguous, uniformly valid approximation across the entire flow field. Numerical results for an insulated plate and a cold plate are presented.

In the sequel of this paper,† the case of $\omega < 1$ will be treated for flows over a flat plate and a $\frac{3}{4}$-powered two-dimensional slender body. The necessity of including the heating and vorticity effect in order to achieve unambiguous uniform validity will be further demonstrated there. Also, by comparing the present paper and its sequel, the influence of the viscosity–temperature law on the flow-field structure can be more clearly understood in detail. Finally we should mention the other higher-order corrections of comparable order of magnitude, due to the slip and

† Presented by the same authors under the title 'Higher-order approximation in the theory of hypersonic boundary layers on slender bodies' in AGARD Seminar on Numerical Methods for Viscous Flows, Teddington, England, September 1967. Manuscript is currently under preparation for publication.

temperature jump effects. By virtue of the linearity of equations governing the higher-order problems, these effects can be studied separately from the heating and vorticity effect. Furthermore, these effects are not connected to the main theoretical concern of the present paper, and hence they are not included here. Also not considered here is the effect of uncertainty about the leading edge, which is assumed to be of still higher order, since we do not encounter any indeterminacy in our analysis.

2. Formulation and analysis

We consider now specifically hypersonic viscous flow over a flat plate (figure 1) of a perfect gas obeying a linear viscosity–temperature law. The non-dimensional governing equations in von Mises's variables are

$$\left.\begin{aligned}
&\frac{\partial}{\partial\psi}\left(\frac{v}{u}\right)-\frac{\partial}{\partial x}\left(\frac{1}{\rho u}\right)=0,\\
&\rho u\frac{\partial u}{\partial x}+\frac{1}{\gamma M_\infty^2}\left(\frac{\partial p}{\partial x}-\rho v\frac{\partial p}{\partial\psi}\right)=\frac{1}{R_\infty}\left\{\rho u\frac{\partial}{\partial\psi}\left[\mu\rho u\frac{\partial u}{\partial\psi}+\mu\left(\frac{\partial v}{\partial x}-\rho v\frac{\partial v}{\partial\psi}\right)\right]\right.\\
&\qquad\left.+\left(\frac{\partial}{\partial x}-\rho v\frac{\partial}{\partial\psi}\right)\left[\tfrac{4}{3}\mu\left(\frac{\partial u}{\partial x}-\rho v\frac{\partial u}{\partial\psi}\right)-\tfrac{2}{3}\mu\rho u\frac{\partial v}{\partial\psi}\right]\right\},\\
&\rho u\left(\frac{\partial v}{\partial x}+\frac{1}{\gamma M_\infty^2}\frac{\partial p}{\partial\psi}\right)=\frac{1}{R_\infty}\left\{\rho u\frac{\partial}{\partial\psi}\left[\tfrac{4}{3}\mu\rho u\frac{\partial v}{\partial\psi}-\tfrac{2}{3}\mu\left(\frac{\partial u}{\partial x}-\rho v\frac{\partial u}{\partial\psi}\right)\right]\right.\\
&\qquad\left.+\left(\frac{\partial}{\partial x}-\rho v\frac{\partial}{\partial\psi}\right)\left[\mu\rho u\frac{\partial u}{\partial\psi}+\mu\left(\frac{\partial v}{\partial x}-\rho v\frac{\partial v}{\partial\psi}\right)\right]\right\},\\
&\rho u\frac{\partial T}{\partial x}-\left(\frac{\gamma-1}{\gamma}\right)u\frac{\partial p}{\partial x}=\frac{1}{\sigma R_\infty}\left\{\rho u\frac{\partial}{\partial\psi}\left(\mu\rho u\frac{\partial T}{\partial\psi}\right)+\left(\frac{\partial}{\partial x}-\rho v\frac{\partial}{\partial\psi}\right)\right.\\
&\qquad\left.\times\left[\mu\left(\frac{\partial T}{\partial x}-\rho v\frac{\partial T}{\partial\psi}\right)\right]\right\}+\frac{(\gamma-1)M_\infty^2}{R_\infty}\mu\left\{\left[\rho u\frac{\partial u}{\partial\psi}+\frac{\partial v}{\partial x}-\rho v\frac{\partial v}{\partial\psi}\right]^2\right.\\
&\qquad\left.+2\left[\left(\frac{\partial u}{\partial x}-\rho v\frac{\partial u}{\partial\psi}\right)^2+\left(\rho u\frac{\partial v}{\partial\psi}\right)^2\right]-\frac{2}{3}\left[\frac{\partial u}{\partial x}-\rho v\frac{\partial u}{\partial\psi}+\rho u\frac{\partial v}{\partial\psi}\right]^2\right\},\\
&\qquad p=\rho T,\quad \mu=CT.
\end{aligned}\right\}\tag{1}$$

The velocity components u and v (parallel and perpendicular to the flat plate respectively), the pressure p, the density ρ, the temperature T and the viscosity μ have been non-dimensionalized with respect to free-stream values. The distances x and y, measured along and perpendicular to the plate, respectively, have been non-dimensionalized with respect to a reference length L. The non-dimensional stream function ψ is related to y by $\partial\psi/\partial y=\rho u$.

The constant parameters appearing in (1) are the Prandtl number σ, the free-stream Mach number $M_\infty\,[=u_\infty\rho_\infty^{\frac{1}{2}}(\gamma\rho_\infty)^{-\frac{1}{2}}]$ and Reynolds number $R_\infty\,[=\rho_\infty u_\infty L/\mu_\infty]$.† To render the results more meaningful, the constant C in the viscosity–temperature law should be determined by using an appropriate reference temperature (see Cheng, Hall, Golian & Hertzberg 1961, for example).

† We adopt largely the symbols used by Bush (1966) for easy comparison with his work.

The free-stream Mach number is considered to be much greater than unity, but its combination with Reynolds number, δ, which represents the order of magnitude of the boundary layer, is considered to be much smaller than unity. Furthermore, in order to confine our study to the strong-interaction problem, we assume that $1/(M_\infty^2\delta^2)$ is much smaller than unity and, for the sake of definiteness, of the order δ^2 or higher. In short, the underlying assumptions of our analysis are

$$M_\infty \gg 1, \quad \delta \equiv [C\gamma M_\infty^2/R_\infty]^{\frac{1}{4}} \ll 1 \quad \text{and} \quad 1/(M_\infty^2\delta^2) = O(\delta^2) \ll 1. \tag{2}$$

In the following, an asymptotic analysis of (1) in terms of the small parameter δ will be made for the inviscid region, a transitional layer and the boundary layer.

The inviscid region

The non-trivial inviscid flow bounded by a strong shock wave is induced by the presence of the boundary layer, whose thickness is of the order δ. According to hypersonic small-disturbance theory, we introduce a set of semi-stretched independent variables and expand the flow quantities as follows:

$$\left.\begin{aligned} x_h = x, \quad \psi_h = \psi/\delta, \\ u-1 = \delta^2[u_h+\epsilon u_{hh}+\ldots], \qquad v = \delta[v_h+\epsilon v_{hh}+\ldots], \\ p = \gamma M_\infty^2\delta^2[p_h+\epsilon p_{hh}+\ldots], \quad T = \gamma M_\infty^2\delta^2[T_h+\epsilon T_{hh}+\ldots], \\ \rho = \rho_h+\epsilon\rho_{hh}+\ldots, \end{aligned}\right\} \tag{3}$$

where $\epsilon \equiv \delta^{2[1-2/(3\gamma)]}$ and the second terms of the expansions are due to the heating and vorticity effect and the displacement effect of the transitional layer. Substituting (3) into (1) yields

$$\left.\begin{aligned} \frac{\partial v_h}{\partial\psi_h} - \frac{\partial}{\partial x_h}\left(\frac{1}{\rho_h}\right) = 0, \quad \rho_h\frac{\partial u_h}{\partial x_h} + \frac{\partial p_h}{\partial x_h} - \rho_h v_h\frac{\partial p_h}{\partial\psi_h} = 0, \\ \frac{\partial v_h}{\partial x_h} + \frac{\partial p_h}{\partial\psi_h} = 0, \quad \rho_h\frac{\partial T_h}{\partial x_h} - \left(\frac{\gamma-1}{\gamma}\right)\frac{\partial p_h}{\partial x_h} = 0, \\ p_h = \rho_h T_h \end{aligned}\right\} \tag{4}$$

and

$$\left.\begin{aligned} \frac{\partial v_{hh}}{\partial\psi_h} + \frac{\partial}{\partial x_h}\left(\frac{\rho_{hh}}{\rho_h^2}\right) = 0, \quad p_{hh} = \rho_h T_{hh} + \rho_{hh} T_h, \\ \frac{\partial v_{hh}}{\partial x_h} + \frac{\partial p_{hh}}{\partial\psi_h} = 0, \quad \rho_h\frac{\partial T_{hh}}{\partial x_h} + \rho_{hh}\frac{\partial T_h}{\partial x_h} - \left(\frac{\gamma-1}{\gamma}\right)\frac{\partial p_{hh}}{\partial x_h} = 0, \\ \rho_h\frac{\partial u_{hh}}{\partial x_h} + \rho_{hh}\frac{\partial u_h}{\partial x_h} + \frac{\partial p_{hh}}{\partial x_h} - \rho_h v_h\frac{\partial p_{hh}}{\partial\psi_h} - (\rho_h v_{hh} + \rho_{hh} v_h)\frac{\partial p_h}{\partial\psi_h} = 0. \end{aligned}\right\} \tag{5}$$

Equations (4) and (5) are the equations of hypersonic small-disturbance theory and their small perturbations, respectively. Four of them can be integrated to yield the Bernoulli equation and the particle isentropic equation and their respective perturbations, as follows:

$$2u_h + v_h^2 + 2\gamma T_h/(\gamma-1) = \text{function}\,(\psi_h), \quad p_h/\rho_h^\gamma = \text{function}\,(\psi_h) \tag{6}$$

and

$$\left.\begin{aligned} u_{hh} + v_h v_{hh} + \gamma T_{hh}/(\gamma-1) = \text{function}\,(\psi_h), \\ p_{hh}/p_h - \gamma\rho_{hh}/\rho_h = \text{function}\,(\psi_h). \end{aligned}\right\} \tag{7}$$

Although the Navier–Stokes equations are our basis of analysis, the inviscid–region approximation up to and including the order considered is purely inviscid, as (4) and (5) show; hence we may consistently consider an infinitesimally thin shock wave governed by the Rankine–Hugoniot conditions. It is known that self-similar solutions exist for (4) and (5) with a power-law shock wave and that the corresponding boundary-layer equations will have a self-similar solution if the power is $\frac{3}{4}$. Thus we assume the shock wave to be described by

$$y_s = \psi_s = \delta A x^{\frac{3}{4}}[1 + \epsilon a x^{-n} + \ldots], \quad n = (1 - 2/3\gamma)/2, \tag{8}$$

where the constants A and a are to be determined. The functions of ψ_h in (6) and (7) can now be evaluated at the shock wave, using the strong Rankine–Hugoniot conditions $[1/(M_\infty^2 \delta^2) = O(\delta^2) \ll 1]$. We assume also the following self-similar transformations:

$$\left.\begin{aligned}
&\zeta_h = \psi_h/(A x_h^{\frac{3}{4}}),\\
&u_h = A^2 x_h^{-\frac{1}{2}} U_h(\zeta_h), \quad u_{hh} = A^2 x_h^{-\frac{1}{2}-n} U_{hh}(\zeta_h),\\
&v_h = A x_h^{-\frac{1}{4}} V_h(\zeta_h), \quad v_{hh} = A x_h^{-\frac{1}{4}-n} V_{hh}(\zeta_h),\\
&p_h = A^2 x_h^{-\frac{1}{2}} P_h(\zeta_h), \quad p_{hh} = A^2 x_h^{-\frac{1}{2}-n} P_{hh}(\zeta_h),\\
&T_h = A^2 x_h^{-\frac{1}{2}} \theta_h(\zeta_h), \quad T_{hh} = A^2 x_h^{-\frac{1}{2}-n} \theta_{hh}(\zeta_h),\\
&\rho_h = D_h(\zeta_h), \quad \rho_{hh} = x_h^{-n} D_{hh}(\zeta_h).
\end{aligned}\right\} \tag{9}$$

Substituting (9) into (4), (5), (6) and (7) then yields two sets of ordinary differential and algebraic equations; they are

$$\left.\begin{aligned}
&V_h' + (\tfrac{3}{4})\zeta_h (1/D_h)' = 0, \quad U_h + V_h^2/2 + \gamma\theta_h/(\gamma - 1) = 0,\\
&P_h' - V_h/4 - 3\zeta_h V_h'/4 = 0, \quad P_h = D_h\theta_h,\\
&P_h/D_h^\gamma = 9[(\gamma - 1)/(\gamma + 1)]^\gamma \zeta_h^{-\frac{2}{3}}/[8(\gamma + 1)],
\end{aligned}\right\} \tag{10}$$

and

$$\left.\begin{aligned}
&V_{hh}' - (\tfrac{3}{4})\zeta_h (D_{hh}/D_h^2)' - nD_{hh}/D_h^2 = 0, \quad P_{hh}/P_h = D_{hh}/D_h + \theta_{hh}/\theta_h,\\
&P_{hh}' - (n + \tfrac{1}{4}) V_{hh} - (\tfrac{3}{4})\zeta_h V_{hh}' = 0, \quad U_{hh} + V_h V_{hh} + \gamma\theta_{hh}/(\gamma - 1) = 0,\\
&P_{hh}/P_h - \gamma D_{hh}/D_h = (\tfrac{8}{3})(1 - n) a \zeta_h^{-\frac{4}{3}n},
\end{aligned}\right\} \tag{11}$$

where the prime denotes differentiation with respect to ζ_h. The necessary boundary conditions are derived from the strong Rankine–Hugoniot conditions as follows:

$$V_h(1) = 3/[2(\gamma + 1)], \quad P_h(1) = 9/[8(\gamma + 1)], \tag{12}$$

and

$$\left.\begin{aligned}
V_{hh}(1) &= a[\tfrac{3}{2}(1 - \tfrac{4}{3}n)/(\gamma + 1) - V_h'(1)],\\
P_{hh}(1) &= a[\tfrac{9}{4}(1 - \tfrac{4}{3}n)/(\gamma + 1) - P_h'(1)],
\end{aligned}\right\} \tag{13}$$

where the terms $V_h'(1)$ and $P_h'(1)$ in (13) result from the expansion of the shock position. For a given value of γ, (10) can now be integrated numerically inward from the shock-wave position in the leading approximation ($\zeta_h = 1$); so can (11) with the unknown constant a scaled out. Thus the inviscid region is solved except for two multiplying factors A and a, which will be determined later by matching.

The solutions of (10) and (11) have singularities at the body ($\zeta_h = 0$). To enable matching with the solutions in the viscous regions and also to aid in the numerical integrations, the asymptotic behaviour of these solutions as ζ_h approaches zero must be investigated. The result is that the flow quantities in the inviscid region behave near the body like

$$\left.\begin{aligned} u-1 &= -\delta^2[A^2\gamma\theta_0/(\gamma-1)]x_h^{-\frac{1}{2}}\zeta_h^{-2/(3\gamma)}+\ldots, \\ v &= \delta A x_h^{-\frac{1}{2}}\{V_0+3\theta_0[2(3\gamma-2)P_0]^{-1}\zeta_h^{1-2/(3\gamma)}+\epsilon x_h^{-n}aV_{00}+\ldots\}, \\ p &= \gamma M_\infty^2\delta^2A^2x_h^{-\frac{1}{2}}[P_0+\epsilon x^{-n}aP_{00}+\ldots], \\ T &= \gamma M_\infty^2\delta^2A^2\theta_0x_h^{-\frac{1}{2}}\zeta_h^{-2/(3\gamma)}+\ldots, \end{aligned}\right\} \tag{14}$$

where the constants $P_0 \equiv P_h(0)$ and $V_0 \equiv V_h(0)$ are determined from integrating (10), the constants $P_{00} \equiv P_{hh}(0)$ and $V_{00} \equiv V_{hh}(0)$ are determined from integrating (11) with $a = 1$, and the constant $\theta_0 = (\gamma-1)P_0/\{(\gamma+1)[8(\gamma+1)P_0/9]^{1/\gamma}\}$. The one-term behaviour for $(u-1)$ and T in (14) comes from U_h and θ_h, respectively. It can be shown that U_{hh} and θ_{hh} behave like $O(\zeta_h^{-2/(3\gamma)-\frac{4}{3}n})$, therefore, we can conclude that the region of validity for the expansions in (3) is $1 \geqslant \zeta_h \gg \delta^3$.

In Oguchi's (1958) work, the higher-order inviscid problem defined by (11) is not solved. Rather, he obtained the constants P_{00} and V_{00} by using the tangent-wedge formula, which is equivalent to evaluating these constants from the shock conditions (13). We shall show later in the section on numerical results that such an approximation may introduce significant errors, especially in the evaluation of V_{00}. Also shown later are Newtonian limit values, which are similarly poor approximations except in cases of γ very close to unity.

The boundary layer

Although the transitional layer is physically next to the inviscid region, it is convenient to deal with the boundary layer first. Here we use a different set of semi-stretched independent variables and expansions as follows:

$$\left.\begin{aligned} &x_b = x = x_h, \quad \psi_b = \psi/\delta^3 = \psi_h/\delta^2, \\ &u = u_b+\epsilon u_{bb}+\ldots, \quad p = \gamma M_\infty^2\delta^2[p_b+\epsilon p_{bb}+\ldots], \\ &v = \delta[v_b+\epsilon v_{bb}+\ldots], \quad T = \gamma M_\infty^2[T_b+\epsilon T_{bb}+\ldots]. \end{aligned}\right\} \tag{15}$$

Note that the order of T and $(u-1)$ assumed in (15) is significantly different from that assumed in (3) for the inviscid region. Substituting (15) into (1) yields

$$\left.\begin{aligned} &\frac{\partial}{\partial\psi_b}\left(\frac{v_b}{u_b}\right) = \frac{\partial}{\partial x_b}\left(\frac{T_b}{u_bp_b}\right), \quad \frac{\partial p_b}{\partial\psi_b} = 0, \\ &\frac{\partial u_b}{\partial x_b}+\frac{T_b}{u_bp_b}\frac{\partial p_b}{\partial x_b} = \frac{\partial}{\partial\psi_b}\left(p_bu_b\frac{\partial u_b}{\partial\psi_b}\right), \\ &\frac{\partial T_b}{\partial x_b}-\left(\frac{\gamma-1}{\gamma}\right)\frac{T_b}{p_b}\frac{\partial p_b}{\partial x_b} = \frac{1}{\sigma}\frac{\partial}{\partial\psi_b}\left(p_bu_b\frac{\partial T_b}{\partial\psi_b}\right)+\left(\frac{\gamma-1}{\gamma}\right)p_bu_b\left(\frac{\partial u_b}{\partial\psi_b}\right)^2, \end{aligned}\right\} \tag{16}$$

and

$$\left.\begin{aligned}
&\frac{\partial}{\partial\psi_b}\left[\frac{v_b}{u_b}\left(\frac{v_{bb}}{v_b}-\frac{u_{bb}}{u_b}\right)\right]+\frac{\partial}{\partial x_b}\left[\frac{T_b}{u_b p_b}\left(\frac{u_{bb}}{u_b}+\frac{p_{bb}}{p_b}-\frac{T_{bb}}{T_b}\right)\right]=0, \quad \frac{\partial p_{bb}}{\partial\psi_b}=0,\\
&\frac{\partial u_{bb}}{\partial x_b}+\frac{T_b}{u_b p_b}\frac{\partial p_{bb}}{\partial x_b}+\left(\frac{u_{bb}}{u_b}+\frac{p_{bb}}{p_b}-\frac{T_{bb}}{T_b}\right)\frac{\partial u_b}{\partial x_b}\\
&\quad=\frac{\partial}{\partial\psi_b}\left\{p_b u_b\left[\frac{\partial u_{bb}}{\partial\psi_b}+\left(\frac{u_{bb}}{u_b}+\frac{p_{bb}}{p_b}\right)\frac{\partial u_b}{\partial\psi_b}\right]\right\}+\left(\frac{u_{bb}}{u_b}+\frac{p_{bb}}{p_b}-\frac{T_{bb}}{T_b}\right)\frac{\partial}{\partial\psi_b}\left(p_b u_b\frac{\partial u_b}{\partial\psi_b}\right),\\
&\frac{\partial T_{bb}}{\partial x_b}+\left(\frac{u_{bb}}{u_b}+\frac{p_{bb}}{p_b}-\frac{T_{bb}}{T_b}\right)\frac{\partial T_b}{\partial x_b}-\left(\frac{\gamma-1}{\gamma}\right)\frac{T_b}{p_b}\left(\frac{\partial p_{bb}}{\partial x_b}+\frac{u_{bb}}{u_b}\frac{\partial p_b}{\partial x_b}\right)\\
&\quad=\frac{1}{\sigma}\left\{\left(\frac{u_{bb}}{u_b}+\frac{p_{bb}}{p_b}-\frac{T_{bb}}{T_b}\right)\frac{\partial}{\partial\psi_b}\left(p_b u_b\frac{\partial T_b}{\partial\psi_b}\right)+\frac{\partial}{\partial\psi_b}\left[p_b u_b\frac{\partial T_{bb}}{\partial\psi_b}+p_b u_b\left(\frac{u_{bb}}{u_b}+\frac{p_{bb}}{p_b}\right)\frac{\partial T_b}{\partial\psi_b}\right]\right\}\\
&\qquad+\left(\frac{\gamma-1}{\gamma}\right)\left\{T_{bb}\frac{p_b u_b}{T_b}\left(\frac{\partial u_b}{\partial\psi_b}\right)^2+2p_b u_b\left[\frac{\partial u_{bb}}{\partial\psi_b}+\left(\frac{u_{bb}}{u_b}+\frac{p_{bb}}{p_b}-\frac{T_{bb}}{T_b}\right)\frac{\partial u_b}{\partial\psi_b}\right]\frac{\partial u_b}{\partial\psi_b}\right\}.
\end{aligned}\right\} \tag{17}$$

Equations (16) are the classical boundary-layer equations. Equations (17) are simply perturbations to (16) and, therefore, do not acquire from (1) additional terms which are absent in (16); equations (17) are homogeneous and the present higher-order boundary-layer problem is different from the classical form (see, for example, Van Dyke 1962).

We observe that the pressure (up to and including the second order) does not change across the boundary layer. It can also be shown that the pressure remains unchanged across the transitional layer. Then, by virtue of matching, the pressure in the boundary layer must be given by (14). We can now assume the following self-similar forms:

$$\left.\begin{aligned}
&\zeta_b=\psi_b/(AP_0^{\frac{1}{2}}x_b^{\frac{1}{4}})=\zeta_h x_h^{\frac{1}{2}}/(\delta^2 P_0^{\frac{1}{2}}),\\
&u_b=U_b(\zeta_b), && u_{bb}=x_b^{-n}U_{bb}(\zeta_b),\\
&v_b=x_b^{-\frac{1}{4}}V_b(\zeta_b)/(AP_0^{\frac{1}{2}}), && v_{bb}=x_b^{-n-\frac{1}{4}}V_{bb}(\zeta_b)/(AP_0^{\frac{1}{2}}),\\
&p_b=A^2P_0x_b^{-\frac{1}{2}}, && p_{bb}=aA^2P_{00}x_b^{-n-\frac{1}{2}},\\
&T_b=\theta_b(\zeta_b), && T_{bb}=x_b^{-n}\theta_{bb}(\zeta_b).
\end{aligned}\right\} \tag{18}$$

The transverse momentum equation in both (16) and (17) is automatically satisfied by the above assumptions. The other equations are transformed into

$$\left.\begin{aligned}
&\left(\frac{V_b}{U_b}\right)'+\frac{\zeta_b}{4}\left(\frac{\theta_b}{U_b}\right)'-\frac{\theta_b}{2U_b}=0,\\
&U_b(U_bU_b')'+\zeta_bU_bU_b'/4+\theta_b/2=0,\\
&\frac{(U_b\theta_b')'}{\sigma}+(\gamma-1)\frac{U_bU_b'^2}{\gamma}+\frac{\zeta_b\theta_b'}{4}-\frac{(\gamma-1)\theta_b}{2\gamma}=0,
\end{aligned}\right\} \tag{19}$$

and

$$\left.\begin{aligned}
&\left[\frac{V_b}{U_b}\left(\frac{V_{bb}}{V_b}-\frac{U_{bb}}{U_b}\right)\right]'-\frac{\zeta_b}{4}\left[\frac{\theta_b}{U_b}\left(\frac{U_{bb}}{U_b}+\frac{aP_{00}}{P_0}-\frac{\theta_{bb}}{\theta_b}\right)\right]'+\frac{1}{3\gamma}\left[\frac{\theta_b}{U_b}\left(\frac{U_{bb}}{U_b}+\frac{aP_{00}}{P_0}-\frac{\theta_{bb}}{\theta_b}\right)\right]=0,\\
&\left(\frac{1}{3\gamma}-\frac{1}{2}\right)U_{bb}-\frac{\zeta_b}{4}U'_{bb}+\left(\frac{1}{3\gamma}-1\right)\frac{aP_{00}\theta_b}{P_0U_b}-\frac{\zeta_b}{4}\left(\frac{U_{bb}}{U_b}+\frac{aP_{00}}{P_0}-\frac{\theta_{bb}}{\theta_b}\right)U'_b\\
&\quad=\left[U_bU'_{bb}+U_bU'_b\left(\frac{U_{bb}}{U_b}+\frac{aP_{00}}{P_0}\right)\right]'+\left(\frac{U_{bb}}{U_b}+\frac{aP_{00}}{P_0}-\frac{\theta_{bb}}{\theta_b}\right)(U_bU'_b)',\\
&\left(\frac{1}{3\gamma}-\frac{1}{2}\right)\theta_{bb}-\frac{\zeta_b}{4}\theta'_{bb}-\frac{\zeta_b}{4}\left(\frac{U_{bb}}{U_b}+\frac{aP_{00}}{P_0}-\frac{\theta_{bb}}{\theta_b}\right)\theta'_b-\left(\frac{\gamma-1}{\gamma}\right)\theta_b\left[\left(\frac{1}{3\gamma}-1\right)\frac{aP_{00}}{P_0}-\frac{U_{bb}}{2U_b}\right]\\
&\quad=\frac{1}{\sigma}\left\{\left(\frac{U_{bb}}{U_b}+\frac{aP_{00}}{P_0}-\frac{\theta_{bb}}{\theta_b}\right)(U_b\theta'_b)'+\left[U_b\theta'_{bb}+\left(\frac{U_{bb}}{U_b}+\frac{aP_{00}}{P_0}\right)U_b\theta'_b\right]'\right\}\\
&\qquad+2\left(\frac{\gamma-1}{\gamma}\right)U_bU'_b\left[\frac{\theta_{bb}U'_b}{2\theta_b}+U'_{bb}+\left(\frac{U_{bb}}{U_b}+\frac{aP_{00}}{P_0}-\frac{\theta_{bb}}{\theta_b}\right)U'_b\right],
\end{aligned}\right\}\tag{20}$$

where the prime denotes differentiation with respect to ζ_b.

The boundary conditions at the flat plate are the no-slip and the constant-temperature conditions, namely,

$$U_b(0)=0,\quad V_b(0)=0,\quad \theta_b(0)=0_{b,w}\tag{21}$$

and

$$U_{bb}(0)=0,\quad V_{bb}(0)=0,\quad \theta_{bb}(0)=0.\tag{22}$$

In the case of an insulated plate, the constant-temperature condition in (21) and (22) must be replaced (but not by $\theta'_b(0)=0$ and $\theta'_{bb}(0)=0$, as explained in the section on numerical results). The special situation is an insulated plate with $\sigma=1$, for which we have the two integrated relations

$$\theta_b=(\gamma-1)(1-U_b^2)/(2\gamma)\tag{23}$$

and

$$\theta_{bb}=-(\gamma-1)U_bU_{bb}/\gamma,\tag{24}$$

which are equivalent to the Crocco relation. In this case, the temperature condition in (21) and (22) is no longer needed.

In order to solve (19) and (20) we need also the boundary conditions on U_b, U_{bb}, θ_b and θ_{bb} as ζ_b approaches infinity. These conditions must be determined by matching; therefore, we have to investigate the asymptotic behaviour of the various quantities. To begin with, we require that U_b approach unity (in order to match) at large ζ_b. Then it can be shown by substitution that at large ζ_b equations (19) give

$$\theta_b=C_1\zeta_b^{-(3\gamma-2)/\gamma}\exp(-\sigma\zeta_b^2/8)[1+K_1/\zeta_b^2+\ldots]+C_2\zeta_b^{2(\gamma-1)/\gamma}[1+\ldots],\tag{25}$$

where C_1 and C_2 are constants of integration and $K_1\equiv-4(3\gamma-2)(2\gamma-1)/(\sigma\gamma^2)$. The behaviour associated with C_2 implies a growing temperature which is incompatible with the matching requirement. Setting C_2 equal to zero is equivalent to enforcing the condition

$$\theta_b\to0\quad\text{as}\quad\zeta_b\to\infty.\tag{26}$$

Likewise, it can be shown that the condition

$$U_b \to 1 \quad \text{as} \quad \zeta_b \to \infty \tag{27}$$

serves to reject the non-decaying behaviour of $(U_b - 1)$ admitted by (19) and insures that at large ζ_b

$$\left.\begin{aligned} U_b &= 1 + D_1 \zeta_b^{-1} \exp(-\zeta_b^2/8)\,[1 + \ldots] \\ &\quad + 8C_1 [\sigma(1-\sigma)]^{-1} \zeta_b^{-(3\gamma-2)/\gamma-2} \exp(-\sigma\zeta_b^2/8)\,[1 + L_1/\zeta_b^2 + \ldots] \quad (\sigma \neq 1), \\ &= 1 + D_1 \zeta_b^{-1} \exp(-\zeta_b^2/8)\,[1 - 4/\zeta_b^2 + \ldots] \\ &\quad - [\gamma C_1/(\gamma-1)]\, \zeta_b^{-(3\gamma-2)/\gamma} \exp(-\zeta_b^2/8)\,[1 + \ldots] \quad (\sigma = 1), \end{aligned}\right\} \tag{28}$$

where D_1 is a constant of integration and

$$L_1 \equiv K_1 + 8[\sigma(1-\sigma)]^{-1}[(5\gamma - 2)(\sigma - \tfrac{1}{2})/\gamma - \sigma/2].$$

It is seen from (23) that D_1 is zero in the case of an insulated plate with $\sigma = 1$. The behaviour of V_b can also be shown by substitution to be

$$V_b = V_b(\infty) + O[\exp(-\zeta_b^2)], \tag{29}$$

where $V_b(\infty)$ is another constant of integration. Conditions (21), (26) and (27) are sufficient to determine the solution of the first-order boundary-layer problem, i.e. (19), including the constants of integration C_1, D_1 and $V_b(\infty)$.

The asymptotic behaviour of the second-order quantities at large ζ_b can be shown by substitution to be the following:

$$\theta_{bb} = E_1 \zeta_b^{-2/(3\gamma)} [1 + K_2/\zeta_b^2 + \ldots] + O[\exp(-\zeta_b^2)], \tag{30}$$

$$U_{bb} = -[\gamma E_1/(\gamma-1)]\, \zeta_b^{-2/(3\gamma)} [1 + L_2/\zeta_b^2 + \ldots] + E_2 \zeta_b^{-4n} [1 + \ldots] + O[\exp(-\zeta_b^2)] \tag{31}$$

and

$$V_{bb} = 3E_1[2(3\gamma-2)]^{-1} \zeta_b^{1-2/(3\gamma)} [1 + O(\zeta^{-1})] + E_3 + O[\exp(-\zeta_b^2)], \tag{32}$$

where E_1, E_2 and E_3 are constants of integration, and $K_2 \equiv 4(3\gamma+2)/(9\sigma\gamma^2)$ and $L_2 \equiv [\gamma(\sigma-1)+1]\, K_2$. Now, by inspection of (14), it is seen that the second-order boundary-layer solution behaves consistently with the inviscid solution near the boundary-layer edge. Although the boundary-layer solution should match formally with the transitional-layer solution, we may, following the practice of previous investigators, tentatively determine the outer-edge boundary conditions for the second-order boundary-layer problem by comparing (14), (30) and (31). Thus we are led to specify that

$$E_1 = A^2 \theta_0 P_0^{-1/(3\gamma)} \quad \text{and} \quad E_2 = 0,$$

or

$$\theta_{bb}\, \zeta_b^{2/(3\gamma)} \to A^2 \theta_0 P_0^{-1/(3\gamma)} \quad \text{as} \quad \zeta_b \to \infty \tag{33}$$

and

$$[U_{bb} + \gamma\theta_{bb}/(\gamma-1)]\, \zeta_b^{4n} \to 0 \quad \text{as} \quad \zeta_b \to \infty. \tag{34}$$

Conditions (22), (33) and (34) are sufficient to determine the solution of the second-order boundary-layer problem, i.e. (20), including the constant of integration E_3. The formal matching of the transitional-layer solution with the inviscid solution and with the boundary-layer solution can be checked *a posteriori*. The as yet unknown constant a appearing in (20) can be scaled out of the integration because of the linearity of these equations and can be determined along with the constant A later in the process of matching.

The transitional layer

The motivation for considering an intermediate transitional layer arises from the established fact that, whereas the first-order boundary-layer temperature decays exponentially, the second-order temperature decays algebraically. Near the outer edge (at large ζ_b), although the combined first- and second-order boundary-layer solution has a proper temperature behaviour to match that of the inviscid flow, the first-order boundary-layer solution already fails to be valid as a first approximation and so possibly would all higher-order boundary-layer solutions. To prove the validity of the combined first- and second-order boundary-layer solution as an asymptotic approximation near the outer edge, one can try to show that the third-order boundary-layer solution remains of higher order. However, a simpler approach is to consider a new set of asymptotic expansions for the region in question.

We note that not only does the temperature undergo transition near the outer edge but also the vorticity $(u-1)$. In the special case of an insulated plate and $\sigma = 1$, these two transitions are the same, but in general they are slightly different [see (25) and (28)]. Fortunately, near the outer edge the energy equation is decoupled from the momentum equation since u is close to unity and hence we may study the two transitions separately.

Consider first the temperature transition. From (25) and (30), we see that T_b ceases to be the asymptotic solution of (1) in the region where

$$\epsilon\zeta_b^{-2/(3\gamma)}/\{\zeta_b^{-(3\gamma-2)/\gamma}\exp[-\sigma\zeta_b^2/8]\} = O(1).$$

To treat this region, we define a new set of independent variables of unit order as follows:

$$x_t = x, \quad \zeta_t = \epsilon\zeta_b^{(9\gamma-8)/(3\gamma)}\exp(\sigma\zeta_b^2/8). \tag{35}$$

The introduction of the last variable is crucial for the success of the subsequent analysis. According to (35), the boundary layer corresponds to a small ζ_t of the order ϵ and the inviscid region corresponds to an exponentially large ζ_t of the order $\exp|O(\delta^{-4})|$. Now, for the sake of convenience, denote the value of ζ_b at $\zeta_t = 1$ as ζ_* so that

$$\zeta_* = [8(\ln 1/\epsilon)/\sigma]^{\frac{1}{2}}\{1-(9\gamma-8)(\ln\ln 1/\epsilon)/[12\gamma(\ln 1/\epsilon)]+\ldots\} \gg 1 \tag{36}$$

and

$$\zeta_b^2 = \zeta_*^2 + [8(\ln\zeta_t)/\sigma][1-8(9\gamma-8)/(6\gamma\sigma\zeta_*^2)+O(1/\zeta_*^4)]. \tag{37}$$

Equation (36) relates the small parameter ϵ or δ to a new large parameter ζ_*, which is logarithmically large in ϵ or δ. From (37), we observe that the transitional layer, where ζ_t is of unit order, is logarithmically far away from the boundary layer, yet its extent $(\zeta_b - \zeta_*)$ is (much) smaller than the boundary layer by a factor of ζ_*^{-1}. For this reason, it is possible to rewrite the inner limit of the inviscid solution (14) into a Taylor expansion for small $(\zeta_h - \delta^2\zeta_* P_0^{\frac{1}{2}}/x_t^{\frac{1}{2}})$.

The flow variables are assumed to have the following expansions:

$$\left.\begin{aligned} v &= \delta[v_t + \epsilon\zeta_*^{1-2/(3\gamma)}(v_{tt} + v_{ttt}/\zeta_*^{1-2/(3\gamma)}) + o(\epsilon)], \\ p &= \gamma M_\infty^2\delta^2[p_t + \epsilon p_{tt} + o(\epsilon)], \\ u &= 1 + o(1), \\ T &= \gamma M_\infty^2\epsilon\zeta_*^{-2/(3\gamma)}[T_t + T_{tt}/\zeta_*^2 + o(\zeta_*^{-2})]. \end{aligned}\right\} \tag{38}$$

In (38), the assumption for u implies that the subsequent results are independent of the $(u-1)$ transition. Also to be noted is the assumption that the temperature in the transitional layer has an order of magnitude intermediate between the inviscid region and boundary-layer temperatures. Substituting (38) into (1) yields

$$\partial p_t/\partial \zeta_t = \partial p_{tt}/\partial \zeta_t = 0, \tag{39}$$

$$\partial v_t/\partial \zeta_t = \partial v_{tt}/\partial \zeta_t = \partial v_{ttt}/\partial \zeta_t = 0, \tag{40}$$

$$\frac{x_t^{\frac{1}{2}}}{A^2 P_0}\zeta_t \frac{\partial}{\partial \zeta_t}\left(p_t \zeta_t \frac{\partial T_t}{\partial \zeta_t}\right) + \zeta_t \frac{\partial T_t}{\partial \zeta_t} = 0, \tag{41}$$

$$\frac{x_t^{\frac{1}{2}}}{A^2 P_0}\zeta_t \frac{\partial}{\partial \zeta_t}\left(p_t \zeta_t \frac{\partial T_{tt}}{\partial \zeta_t}\right) + \zeta_t \frac{\partial T_{tt}}{\partial \zeta_t} = \frac{16 x_t}{\sigma}\left\{\left(\frac{\partial}{\partial x_t} + \frac{9\gamma - 8}{12\gamma x_t}\zeta_t \frac{\partial}{\partial \zeta_t}\right) T_t - \frac{p_t}{4A^2 P_0 x_t^{\frac{1}{2}}}\zeta_t \frac{\partial T_t}{\partial \zeta_t} - \left(\frac{\gamma - 1}{\gamma}\right)\frac{T_t}{p_t}\frac{\partial p_t}{\partial x_t}\right\}. \tag{42}$$

Equations (39) merely confirm the statement made in the boundary-layer analysis that the pressure remains unchanged across the transitional layer. Equations (40) show that the transverse velocity also remains unchanged. The constants A and a can now be determined by matching the inviscid behaviour of v in (14) to the boundary-layer behaviour. The results are

$$A = [V_b(\infty)/(V_0 P_0^{\frac{1}{2}})]^{\frac{1}{2}} \tag{43}$$

and

$$a = E_3/(V_{00} A^2 P_0^{\frac{1}{2}}) = E_3 V_0/[V_{00}\, V_b(\infty)]. \tag{44}$$

The solution of (41) has the general form

$$T_t = f_1(x_t)/\zeta_t + f_2(x_t).$$

Now, the inner limit of the inviscid solution to be matched is the expansion of (14) in the vicinity of $\zeta_h = \delta^2 \zeta_* P_0^{\frac{1}{2}}/x_t^{\frac{1}{2}}$, for the reason noted earlier. The matching at large ζ_t is thus accomplished by setting $f_2(x_t) = A^2 \theta_0 P_0^{-1/(3\gamma)} x_t^{-n}$, and the matching at small ζ_t with the boundary-layer solution is accomplished by setting $f_1(x_t) = C_1$. In short, we have

$$T_t = C_1/\zeta_t + A^2 \theta_0 P_0^{-1/(3\gamma)} x_t^{-n}. \tag{45}$$

On the right-hand side of (45), the first term corresponds to the outer limit of the first-order boundary-layer solution; and the second term to that of the second-order boundary-layer solution. It is clear now that in the transitional layer the two boundary-layer solutions are equally important and hence the consideration of the second-order boundary layer is necessary. In a similar manner, we can show that the solution of (42), which also fulfils all matching requirements, is

$$T_{tt} = [K_1 - 8(\ln \zeta_t)/(3\gamma\sigma)]\,(C_1/\zeta_t) + [K_2 - 8(\ln \zeta_t)/(3\gamma\sigma)]\, A^2 \theta_0 P_0^{-1/(3\gamma)} x_t^{-n}. \tag{46}$$

Comparing (45) and (46) we conclude that the region of validity for the transitional-layer solution (for the first-order solution at least) is $\exp|O(\zeta_*^2)| \gg \zeta_t \gg \exp[-|O(\zeta_*^2)|]$. Thus the overlapping region of validity of the transitional-layer and the boundary-layer solution is $1 \gg \zeta_t \gg \exp[-|O(\zeta_*^2)|]$ and that of the transitional-layer and inviscid solution is $\exp|O(\zeta_*^2)| \gg \zeta_t \gg 1$. Finally, we note that the first- and second-order transitional-layer solution is exactly the two-

term outer limit of the first- and second-order boundary-layer solution. In other words, the first- and second-order boundary-layer solution is the composite expansion for both the transitional and the boundary layer; therefore, the validity of the combined first- and second-order boundary-layer solution near the outer edge as an asymptotic solution of (1) is proved.

Next, let us examine the transition of $(u-1)$. Because of the different behaviour of U_b at large ζ_b for different Prandtl number and plate conditions, the various cases must be discussed separately. The most trivial case is an insulated plate with $\sigma = 1$. The behaviour of $(u-1)$ is locked to that of T by (23) and (24) and we can prove that in the transitional layer

$$u = 1 - \epsilon\zeta_*^{-2/(3\gamma)}[\gamma/(\gamma-1)][T_t + T_{tt}/\zeta_*^2 + \ldots]. \tag{47}$$

In the case of $\sigma < 1$, the transition of $(u-1)$ occurs slightly ahead of that of T (as $\zeta_b \to \infty$), in a region where the variable

$$\bar{\zeta}_t = \zeta_t \zeta_*^2 [1 + \ldots] \tag{48}$$

is of unit order. In this region, the temperature can be found, from either (45) and (46) or the boundary-layer solution, to be

$$T = \gamma M_\infty^2 \epsilon\zeta_*^{2-2/(3\gamma)}\{C_1/\bar{\zeta}_t + [C_1/(\bar{\zeta}_t\zeta_*^2)][(8/\sigma)(1-[1/3\gamma])(\ln\bar{\zeta}_t - 2\ln\zeta_*) + K_1] + A^2\theta_0 P_0^{-1/(3\gamma)} x_t^{-n}/\zeta_*^2 + \ldots. \tag{49}$$

Then, from the streamwise-momentum equation of (1), we can obtain the transitional-layer solution for u, in the same way as that for T, namely

$$u = 1 + \epsilon\zeta_*^{-2/(3\gamma)}\left\{\frac{8C_1}{\sigma(1-\sigma)\bar{\zeta}_t} - \frac{\gamma A^2\theta_0 P_0^{-1/(3\gamma)}}{\gamma-1} x_t^{-n} + \frac{1}{\zeta_*^2}\left[\frac{8C_1L_1}{\sigma(1-\sigma)\bar{\zeta}_t} - \frac{\gamma A^2\theta_0 P_0^{-1/(3\gamma)} L_2}{\gamma-1} x_t^{-n} - \frac{8}{3\gamma\sigma}\left(\frac{8C_1}{\sigma(1-\sigma)\bar{\zeta}_t} - \frac{\gamma A^2\theta_0 P_0^{-1/(3\gamma)}}{\gamma-1} x_t^{-n}\right)(\ln\bar{\zeta}_t - 2\ln\zeta_*^2)\right]\right\} + \ldots. \tag{50}$$

In the case of an non-insulated plate with $\sigma = 1$, the transition of $(u-1)$ occurs slightly behind that of T, in a region where the variable

$$\tilde{\zeta}_t = \zeta_t \zeta_*^{-2(\gamma-1)/\gamma}[1 + \ldots] \tag{51}$$

is of unit order. In this region, the temperature has already undergone its transition, and can be found to be

$$T = \gamma M_\infty^2 \epsilon\zeta_*^{-2/(3\gamma)} A^2\theta_0 P_0^{-1/(3\gamma)} x_t^{-n} + \ldots. \tag{52}$$

It can be shown that in this case we have

$$u = 1 + \epsilon\zeta_*^{-2/(3\gamma)}\left\{\frac{D_1}{\tilde{\zeta}_t} - \frac{\gamma A^2\theta_0 P_0^{-1/(3\gamma)}}{\gamma-1} x_t^{-n} - \frac{\gamma C_1}{(\gamma-1)\tilde{\zeta}_t\zeta_*^{2(\gamma-1)/\gamma}} + \frac{1}{\zeta_*^2}\left[-\frac{4D_1}{\tilde{\zeta}_t} - \frac{\gamma A^2\theta_0 P_0^{-1/(3\gamma)} L_2}{\gamma-1} x_t^{-n} - \frac{8}{3\gamma\sigma}\left(\frac{D_1}{\tilde{\zeta}_t} - \frac{\gamma A^2\theta_0 P_0^{-1/(3\gamma)} x_t^{-n}}{\gamma-1}\right) \times \left(\ln\tilde{\zeta}_t + 2\frac{\gamma-1}{\gamma}\ln\zeta_*\right)\right] + \ldots\right\}. \tag{53}$$

We will not discuss in detail the cases of $\sigma > 1$.

In summary, we find that in any case the transitional-layer solution for $(u-1)$ is again exactly the outer limit of the two-term boundary-layer expansion.

3. Numerical results

In the foregoing, the problem of hypersonic strong interaction has been reduced to sets of ordinary differential equations with well-defined boundary conditions. These equations must be integrated numerically. To illustrate some of the non-trivial details of this procedure and the resulting magnitude of the heating and vorticity effect, we treat here two cases: (i) an insulated plate with $\sigma = 1$, and (ii) a cold plate with $\theta_{b,w} = 0{\cdot}1(\gamma-1)/\gamma$ and $\sigma = \frac{3}{4}$. For both cases, results are obtained for γ equal to $\frac{7}{5}$ and $\frac{5}{3}$.

The inviscid equations (10) and (11) are integrated first. The integration from the primary position of shock ($\zeta_h = 1$) to the equivalent body ($\zeta_h = 0$) is straightforward, except that the singularity at $\zeta_h = 0$ tends to promote severe numerical inaccuracies in its vicinity. To remedy this difficulty, we integrate in terms of a transformed independent variable $\bar{\zeta}_h = \zeta_h^{(3\gamma-2)/(9\gamma)}$; the singularity is thus rendered much weaker, if not removed. The resulting numerical values for the constants P_0, V_0, θ_0, P_{00} and V_{00} are listed in table 1. In this table the values corresponding to the Newtonian limit are shown for comparison. Generally, the Newtonian values are seen to give a better approximation for the pressure than for

γ	P_0	V_0	θ_0	P_{00}	V_{00}
$\frac{5}{3}$	0·24017	0·35945	0·084189	0·12818 (0·26016)	−0·42938 (0·19688)
$\frac{7}{5}$	0·27947	0·44340	0·067394	0·19536 (0·37574)	−0·39345 (0·30257)
1 (Newtonian)	0·37500	0·75000	—	0·44444	0·58333

TABLE 1

the transverse velocity, and a better approximation for the first-order quantities than for the second-order quantities. In particular, the exact numerical results yield negative values for V_{00}, which mean an equivalent-body perturbation in the opposite direction of the shock-wave perturbation, contrary to the Newtonian result. While this disparity in the perturbations is perhaps unexpected by intuition, it is physically explainable, since the inward perturbation of the equivalent body actually makes a more blunt-nosed body. This produces a stronger shock near the leading edge, a less dense gas in the shock layer and an outward perturbation of the shock-wave shape. For values of γ sufficiently close to unity, this disparity disappears and the Newtonian limit becomes a better approximation. The fact is borne out by exact calculation for $\gamma = 1{\cdot}10$, which gives $P_{00} = 0{\cdot}35245$ and $V_{00} = 0{\cdot}05396$, and exact calculation for $\gamma = 1{\cdot}01$, which gives $P_{00} = 0{\cdot}43387$ and $V_{00} = 0{\cdot}51022$. Also shown parenthetically are the

values of P_{00} and V_{00}, calculated by using the shock condition (13), which is equivalent to Oguchi's use of the tangent-wedge formula. It is apparent that the use of the tangent-wedge formula is not a good approximation in the second-order problem and should be avoided.

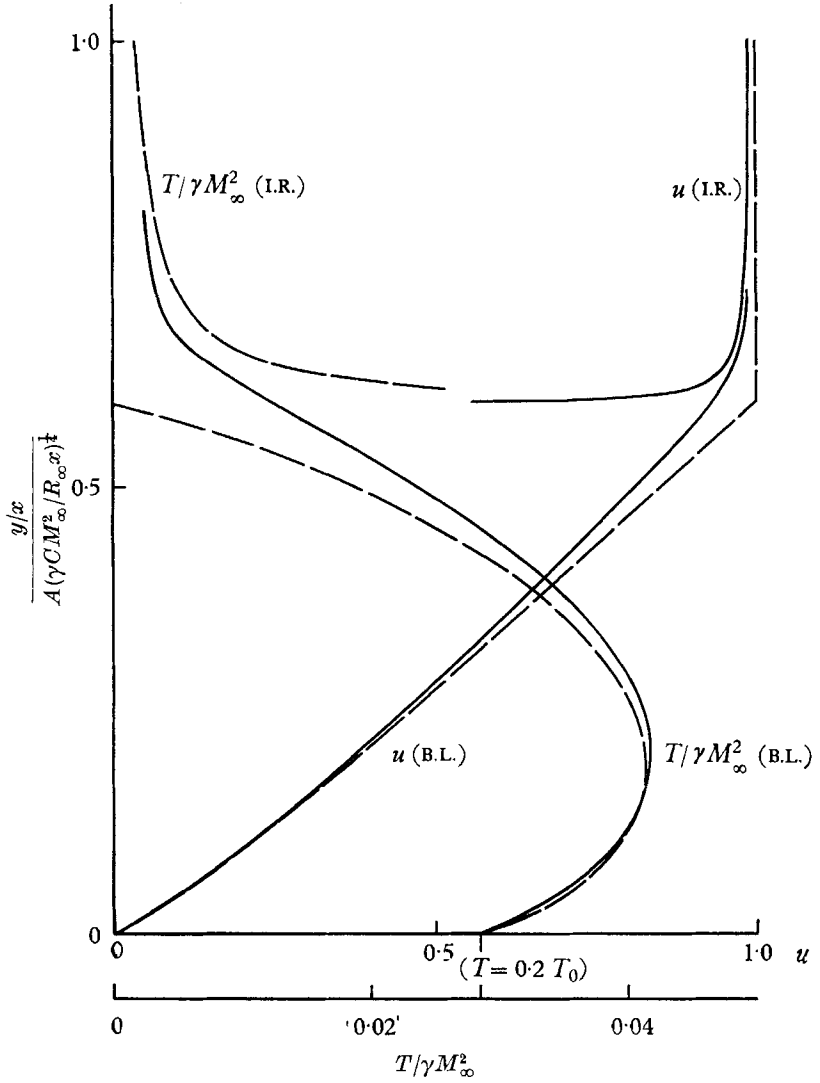

FIGURE 2. Typical streamwise velocity and temperature profiles; $\theta_{b,w} = 0{\cdot}1(\gamma-1)/\gamma$, i.e. $T_w/T_0 = 0{\cdot}2$, $\gamma = \frac{7}{5}$; $\sigma = \frac{3}{4}$; $\epsilon x^{-[1-2/(3\gamma)]/2} \equiv [(C\gamma M_\infty^2)/(R_\infty x)]^{[1-2/(3\gamma)]/2} = 0{\cdot}2$. Dashed curves are first approximations and solid curves are second approximations. (B.L.) stands for the boundary layer and (I.R.) stands for the inviscid region.

The boundary-layer equations (19) and (20) are integrated from the plate ($\zeta_b = 0$) toward the outer edge ($\zeta_b \to \infty$). Since this is a two-point boundary-value problem, the integration involves guessing of certain initial values at $\zeta_b = 0$.

Because of the singularity at $\zeta_b = 0$, the integrations are started with the help of the following asymptotic series:

$$\left.\begin{aligned} U_b &= \alpha_{11}\zeta_b^{\frac{1}{2}} + \alpha_{12}\zeta_b + \alpha_{13}\zeta_b^{\frac{3}{2}} + \ldots, \\ U_{bb} &= \alpha_{21}\zeta_b^{\frac{1}{2}} + \alpha_{22}\zeta_b + \alpha_{23}\zeta_b^{\frac{3}{2}} + \ldots, \\ \theta_b &= \alpha_{30} + \alpha_{31}\zeta_b^{\frac{1}{2}} + \alpha_{32}\zeta_b + \alpha_{33}\zeta_b^{\frac{3}{2}} + \ldots, \\ \theta_{bb} &= \alpha_{40} + \alpha_{41}\zeta_b^{\frac{1}{2}} + \alpha_{42}\zeta_b + \alpha_{43}\zeta_b^{\frac{3}{2}} + \ldots, \\ V_b &= \alpha_{52}\zeta_b + \alpha_{53}\zeta_b^{\frac{3}{2}} + \alpha_{54}\zeta_b^{2} + \ldots, \\ V_{bb} &= \alpha_{62}\zeta_b + \alpha_{63}\zeta_b^{\frac{3}{2}} + \alpha_{64}\zeta_b^{2} + \ldots. \end{aligned}\right\} \tag{54}$$

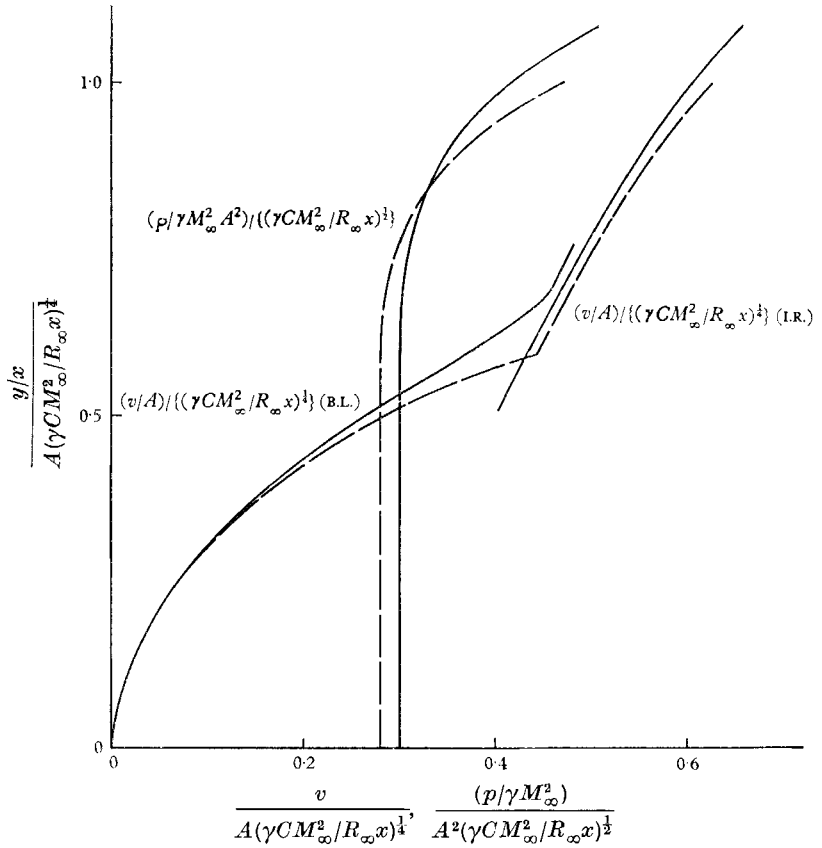

FIGURE 3. Typical transverse velocity and pressure profiles; $\theta_{b,w} = 0{\cdot}1(\gamma-1)/\gamma$, i.e. $T_w/T_0 = 0{\cdot}2$; $\gamma = \frac{7}{5}$; $\sigma = \frac{3}{4}$; $\epsilon x^{-[1-2/(3\gamma)]/2} \equiv [(C\gamma M_\infty^2)/(R_\infty x)]^{[1-2/(3\gamma)]/2} = 0{\cdot}2$. Dashed curves are first approximations and solid curves are second approximations. (B.L.) stands for the boundary layer and (I.R.) stands for the inviscid region.

For a constant-temperature plate, α_{30} is $\theta_{b,w}$ and α_{40} is zero, as specified by (21), but trial values for α_{11}, α_{21}, α_{31} and α_{41} must be used to meet the conditions (26), (27), (33) and (34). For an insulated plate, α_{31} and α_{41} are zero and the proper values for α_{11}, α_{21}, α_{30} and α_{40} must be obtained by trial. The remaining α's can be determined by the differential equations in terms of the given and the trial α's. Once the solution of (19) is obtained, the constant A can be determined from

(43). The solution of (20) involves the simultaneous determination of the constant a by using (44). The linearity of (20) can be exploited to reduce the task of guessing the initial values and value for a. The details need not be given here.

For graphical illustration we present in figures 2 and 3 the numerical results for the case of a cold plate with $\gamma = \frac{7}{5}$. In both figures, the dashed curves represent the first approximations, corresponding to Stewartson's (1955) analysis, and the solid curves represent the second approximations, including the effects associated with shock heating and external vorticity. It is obvious that the

	Q_1				Q_2			
	Insulated plate		Cold plate		Insulated plate		Cold plate	
Q	$\gamma = \frac{5}{3}$	$\gamma = \frac{7}{5}$	$\gamma = \frac{5}{3}$	$\gamma = \frac{7}{5}$	$\gamma = \frac{5}{3}$	$\gamma = \frac{7}{5}$	$\gamma = \frac{5}{3}$	$\gamma = \frac{7}{5}$
$y_s/(x\delta_1)$	1·637	1·189	1·052	0·772	0·5065	0·5016	0·559	0·570
$p/(M_\infty^2\delta_1^2)$	1·074	0·5534	0·444	0·233	0·2703	0·3506	0·298	0·398
C_f/δ_1^3	0·8852	0·5672	0·412	0·281	−0·1770	−0·0475	−0·152	−0·036
C_H/δ_1^3	—	—	0·164	0·118	—	—	−0·089	−0·021

TABLE 2

second approximations improve the matching between the inviscid solution and the boundary-layer solution. The remaining discrepancies between them will be reduced if smaller values of $\epsilon x^{-[1-2/(3\gamma)]/2}$ are used. The numerical results substituted into (8) and (14) give explicit formulas for the shock-wave shape and the surface pressure. Corresponding expressions can also be obtained for the skin-friction coefficient $C_f \equiv 2\bar{\mu}(\partial\bar{u}/\partial\bar{y})/(\rho_\infty\bar{u}_\infty^2)$ and, in the case of a cold plate, the surface-heat-transfer coefficient $C_H \equiv k(\partial\bar{T}/\partial\bar{y})/[\bar{\rho}_\infty\bar{u}_\infty(\bar{H}_\infty - \bar{H}_w)]$, where the barred quantities are dimensional and k and H denote the coefficient of heat conductivity and the total enthalpy respectively. In short, we have

$$Q = Q_1\{1 + Q_2[\delta_1(x)]^{2-4/(3\gamma)}\}, \tag{55}$$

where Q refers to a physical quantity, $\delta_1(x) \equiv [(M_\infty^2 C)/(R_\infty x)]^{\frac{1}{2}}$, and Q_1 and Q_2 are numbers from the numerical results and are listed in table 2.

The second term in (55) represents the correction due to the effects associated with shock heating and external vorticity. Since there is no characteristic geometrical length in this problem, it is obvious that the final results expressed by (55) are independent of the choice of reference length L. The product $M_\infty^2\delta_1^2$ is identical to $\bar{\chi}$ used in the literature.

From the results, we see that the effects associated with shock heating and external vorticity displace the shock wave outward and increase the surface pressure as also illustrated in figure 3. On the other hand, contrary to the common belief, these effects result in a reduction of the skin friction and the surface heat transfer. It may be pointed out that a simplified physical reasoning, based on considering the temperature increase at the boundary-layer edge alone, would lead to the conclusion of an increase in the surface heat transfer. A clearer picture

can be seen from the typical boundary-layer velocity and temperature profiles presented in figure 2. We observe that these effects so displace the streamlines as to stretch the profiles, and hence to cause a net reduction of the skin friction and the surface heat transfer. Also, the streamlines are displaced outward in the outer part of the boundary layer and more so near the edge. This explains the comparatively large effect on the shock-wave shape and the pressure.

4. Concluding remarks

In the hypersonic strong-interaction problem, because of the effects of shock heating and external vorticity, there exists between the inviscid region and the boundary layer an intermediate transitional layer which is not present in the classical boundary-layer theory. For the case of $\mu \propto T$, an asymptotic analysis of the Navier–Stokes equations shows that the analysis of the transitional layer can be avoided by using von Mises's variables or variables for a similar nature as those used by Oguchi (1958), because the first-order boundary-layer solution combined with its second-order correction is proved to be the valid asymptotic solution for both the transitional and the boundary layer. It is also shown that the second-order boundary-layer problem, not considered by Bush (1966), must be treated in order to have an unambiguous, uniformly valid temperature distribution across the entire flow field. This point will be further demonstrated in the analysis of cases of $\mu \propto T^{\omega}$ ($\omega < 1$) which, compared with the present analysis, will also bring out in detail the influence of the viscosity–temperature law on the flow field structure.

Numerical results have been obtained for an insulated plate with $\sigma = 1$ and a cold plate with $\sigma = \frac{3}{4}$. We have demonstrated that the use of tangent-wedge approximation in the second-order problem introduces large numerical errors for either $\gamma = \frac{5}{3}$ or $\gamma = \frac{7}{5}$, and should be avoided. The numerical results show that the effects associated with shock heating and external vorticity influence primarily the outer part of the boundary layer and the inviscid region, hence the shock-wave shape and the pressure distribution. The influence of these effects on the skin friction and the surface heat transfer is numerically small. Since the other second-order effects of comparable importance, those due to slip and temperature jump, have been shown to have no effect on the surface heat transfer (Aroesty 1964), we may conclude from the present analysis that the first-order theoretical results for the surface heat transfer should be quite satisfactory in comparison with experimental results. However, the comparison of the other quantities in theory and in experiment should include the effects due to slip and temperature jump which have not been considered here.

The authors wish to thank Dr W. B. Bush and Dr H. Oguchi for their discussions and Mr W. W. Tieman for programming the numerical calculations. An abstract of this work was presented to the Twelfth International Congress of Applied Mechanics in Stanford, California, August 1968. The work was supported by the Douglas Independent Research and Development (IRAD) Program, to which one of us (H. K. C.) is a consultant.

REFERENCES

AROESTY, J. 1964 Slip flow and hypersonic boundary layers. *AIAA J.* **2**, 189.

BUSH, W. B. 1966 Hypersonic strong-interaction similarity solutions for flow past a flat plate. *J. Fluid Mech.* **25**, 51.

CHENG, H. K., HALL, J. G., GOLIAN, T. C. & HERTZBERG, A. 1961 Boundary-layer displacement and leading-edge bluntness effects in high-temperature hypersonic flow. *J. aeronaut. Sci.* **28**, 353.

LEES, L. 1953 On the boundary-layer equations in hypersonic flow and their approximate solutions. *J. aeronaut. Sci.* **20**, 143.

LEES, L. 1956 Influence of the leading-edge shock waves on the laminar boundary layer at hypersonic speeds. *J. aeronaut. Sci.* **23**, 594.

MATVEEVA, N. S. & SYCHEV, V. V. 1965 On the theory of strong interaction of the boundary layer with an inviscid hypersonic flow. *PMM* **29**, 644.

OGUCHI, H. 1958 First-order approach to a strong interaction problem in hypersonic flow over an insulated flat plate. *Aeronautical Research Institute University of Tokyo*, Report no. 330.

STEWARTSON, K. 1955 On the motion of a flat plate at high speeds in a viscous compressible fluid, II. Steady motion. *J. aeronaut. Sci.* **22**, 303.

VAN DYKE, M. D. 1962 Higher approximations in boundary-layer theory. Part 1. General analysis. *J. Fluid Mech.* **14**, 161.